7-2011

Reconstructed Fermi Surface of Underdoped Bi2Sr2CaCu2O8+δ Cuprate Superconductors

H.-B. Yang
Brookhaven National Laboratory

J. D. Rameau
Brookhaven National Laboratory

See next page for additional authors

Reconstructed Fermi Surface of Underdoped $Bi_2Sr_2CaCu_2O_{8+\delta}$ Cuprate Superconductors

H.-B. Yang,[1] J. D. Rameau,[1] Z.-H. Pan,[1] G. D. Gu,[1] P. D. Johnson,[1] H. Claus,[2] D. G. Hinks,[2] and T. E. Kidd[3]

[1]*Condensed Matter Physics and Materials Science Department, Brookhaven National Laboratory, Upton, New York 11973, USA*

[2]*Materials Science Division, Argonne National Laboratory, Argonne, Illinois 60439, USA*

[3]*Physics Department, University of Northern Iowa, Cedar Falls, Iowa 50614, USA*

(Received 6 August 2010; published 20 July 2011)

The Fermi surface topologies of underdoped samples of the high-T_c superconductor $Bi_2Sr_2CaCu_2O_{8+\delta}$ have been measured with angle resolved photoemission. By examining thermally excited states above the Fermi level, we show that the observed Fermi surfaces in the pseudogap phase are actually components of fully enclosed hole pockets. The spectral weight of these pockets is vanishingly small at the magnetic zone boundary, creating the illusion of Fermi ''arcs.'' The area of the pockets as measured in this study is consistent with the doping level, and hence carrier density, of the samples measured. Furthermore, the shape and area of the pockets is well reproduced by phenomenological models of the pseudogap phase as a spin liquid.

DOI: 10.1103/PhysRevLett.107.047003 PACS numbers: 74.25.Jb, 71.18.+y, 74.72.Kf, 79.60.−i

Understanding the pseudogap regime in the high-T_c superconducting cuprates is thought to be key to understanding the high-T_c phenomenon in general [1]. An important component of that understanding will be the determination of the nature of the low lying normal state electronic excitations that evolve into the superconducting state. It is therefore critically important to know the exact nature of the Fermi surface (FS). Photoemission studies of the pseudogap regime reveal gaps in the spectral function in directions corresponding to the copper-oxygen bonds and a FS that seemingly consists of disconnected arcs falling on the FS defined within the framework of a weakly interacting Fermi liquid [2]. A number of different theories have attempted to explain these phenomena in terms of competing orders whereby the full FS undergoes a reconstruction reflecting the competition [3,4]. An alternative approach recognizes that the superconducting cuprates evolve with doping from a Mott insulating state with no low energy charge excitations to a new state exhibiting properties characteristic of both insulators and strongly correlated metals.

Several theories have been proposed to describe the cuprates from the latter perspective [5–7]. One such approach is represented by the so-called Yang-Rice-Zhang (YRZ) ansatz [6], which, based on the doped resonant valence bond (RVB) spin liquid concept [8], has been shown to successfully explain a range of experimental observations in the underdoped regime [9–12]. The model is characterized by two phenomena, a pseudogap that differs in origin from the superconducting gap and hole pockets that satisfy the Luttinger sum rule for a FS defined by both the poles and zeros of Green's function at the chemical potential [13]. The pockets manifest themselves along part of the FS as an ''arc'' possessing finite spectral weight corresponding to the poles of Green's function as in a conventional metal. The remaining ''ghost'' component of the FS is defined by the zeros of Green's function and therefore possesses no spectral weight to be directly observed. Importantly, the zeros of Green's function at the chemical potential coincide with the magnetic zone boundary associated with the underlying antiferromagnetic (AFM) order of the Mott insulating state and therefore restrict the pockets to lying on only one side of this line. The model further predicts that the arc and ghost portions of the FS are smoothly connected into pockets. Several theoretical studies indicate that within this framework the pockets have an area that scales with the doping [6,10]. Recent photoemission studies have indeed provided some indication that the pseudogap regime is characterized by hole pockets centered in the nodal direction [14,15]. Furthermore, the possibility that FS in the underdoped materials consists of a pocket structure is at the heart of the interpretation of recent studies that identified quantum oscillations in these materials [16]. In the present study, we demonstrate for the first time that the FS of the underdoped cuprates in the normal state is characterized by hole pockets with an area proportional to the doping level.

The photoemission studies reported in this Letter were carried out on underdoped cuprate samples, both Ca doped and oxygen deficient. The Ca-rich crystal was grown from a rod with $Bi_{2.1}Sr_{1.4}Ca_{1.5}Cu_2O_{8+\delta}$ composition using an arc-image furnace with a flowing 20% O_2-Ar gas mixture. The maximum T_c was 80 K. The sample was then annealed at 700 °C giving a 45 K T_c with a transition width of 2 K. The oxygen-deficient $Bi_2Sr_2CaCu_2O_{8+\delta}$ (Bi2212) crystals were produced by annealing optimally doped Bi2212 crystals, at 450 °C to 650 °C for 3–15 days. The spectra shown in this Letter were all recorded on beam line U13UB at the NSLS using a Scienta SES2002 electron spectrometer. Each spectrum was recorded in the pulse-counting mode with an energy and angular resolution of 15 meV and 0.1°, respectively.

Figures 1(a)–1(f) show photoemission spectra obtained near the end of the measured "Fermi arc" for an underdoped Bi2212 ($T_c = 65$ K) sample. The spectra in Figs. 1(g)–1(l) are shown after analysis using the Lucy-Richardson deconvolution approach [17] to reduce the effects of the experimental resolution and after division by the appropriate temperature dependent Fermi function. This approach allows a more accurate determination of the FS crossings [18]. The spectrum in Fig. 1(m) contains two experimental observations as indicated in the schematic in Fig. 1(o), the directly measured FS crossing, point A, and the point at which the dispersion comes to an abrupt halt, point B. We associate the point B with a gap in the spectral function reflecting the scattering of the photohole in the underlying spin liquid. As noted earlier, several calculations indicate that the formation of a Fermi hole pocket reflecting a particle-hole asymmetry in binding energy is derived from this scattering [5,6]. Alternative models that recognize the strong correlations in the system can also produce pockets [7,19]. Within the YRZ ansatz, the pocket in Fig. 1(p) is formed by two band crossings, points A and C in Fig. 1(o), symmetric about the zone point associated with the bottom of the gap derived from the scattering, point B. The Fermi pocket derived in this manner is compared in the figure with the full FS traditionally assumed in angle-resolved photoemission spectroscopy (ARPES) studies and as found from symmetrizing that data as indicated. The deviation between the latter FS and that determined in the present study becomes most evident near the end of the arc. It is important to note that the hole pocket determined in this manner is clearly asymmetric with respect to the magnetic zone boundary, ruling out any pockets generated by scattering mechanisms simply associated with a $Q(\pi, \pi)$ vector, that might for instance reflect commensurate long range AFM order. Of course, the asymmetry may reflect incommensurate or short range AFM order. The ghost portion of the FS is, however, consistent with models showing a surface of zeros in Green's function at the chemical potential running along the magnetic zone boundary [6]. Under the condition $G(\vec{k}, \omega) = 0$, the spectral weight measurable by photoemission is vanishingly small because the spectral function is defined by $A(\vec{k}, \omega) = -\mathrm{Im}G(\vec{k}, \omega)$.

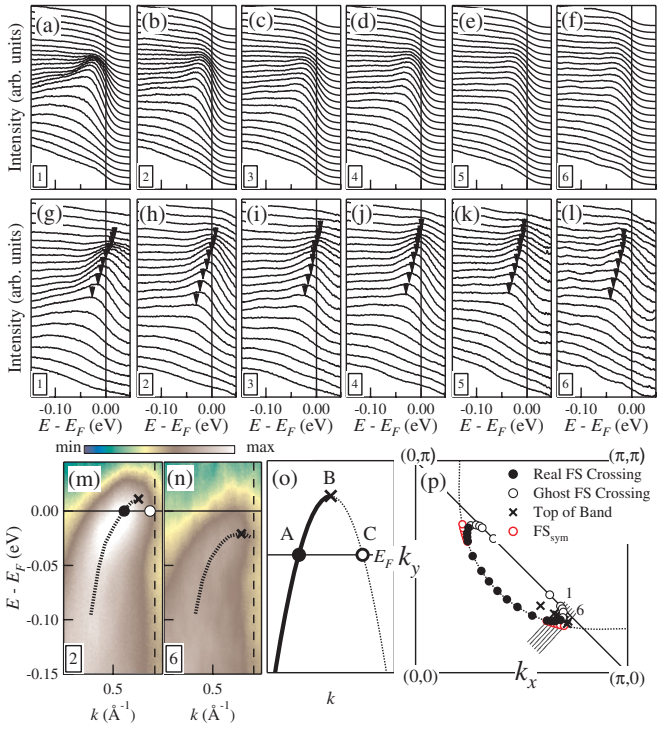

FIG. 1 (color online). Fermi surface of underdoped Bi2212 at 140 K ($T_c = 65$ K). (a)–(f) Energy distribution curves (EDCs) of raw data taken at cuts 1–6 in (p), and (g)–(l) after the analysis described in the text. The EDC peak positions are marked with triangles. FS crossing points exist in cuts 1–4, but not in cuts 5 and 6. (m) Image plot of cut 2 after Fermi normalization, with the FS crossing (solid circle) and the top of the band (cross) indicated. The ghost FS crossing (open circle) deduced from symmetrization in momentum is also indicated. The dashed line represents the location of the magnetic zone boundary. (n) The same image plot for cut 6 showing no FS crossing. (o) Schematic showing points analyzed in the measured spectra as indicated in the text. (p) Pseudopocket determined for the 65 K sample. Black solid circles indicate the measured FS crossings corresponding to point A in the schematic. Crosses show the measured extremity of the dispersion corresponding to point B, and black open circles represent the ghost FS corresponding to point C. Red open circles are the FS crossings obtained from symmetrization. The dashed line indicates the large FS by LDA.

Having determined the approximate shape and size of the pocket we can calculate the associated hole density for a given sample. Assuming the area inside the magnetic zone boundary corresponds to one electron at half filling, the pocket area corresponds to a hole carrier density of 0.15, higher than the doping level determined from the measured T_c alone. However, the measured area is in reasonably good agreement with the area bounded by the locus of superconducting Bogoliubov band minima $k_B(E)$ extracted from spectroscopic imaging scanning tunneling spectroscopy (SISTS) studies of a sample with a similar doping level [20]. The combination of the two experiments raises obvious questions. Does the pocket area really scale with the doping level, and how is that consistent with earlier studies suggesting the arc length is temperature dependent with a length proportional to T/T^* [21]? (Here T^* represents the doping dependent pseudogap temperature scale.) In attempting to answer these questions we show in Fig. 2(a) a comparison of the FSs obtained using the present approach for the 65 K sample, a Ca doped sample ($T_c = 45$ K), and an oxygen-deficient nonsuperconducting sample ($T_c = 0$ K). It is clear from Fig. 2(a) that reducing the doping level into the highly underdoped regime results in a more noticeable deviation from the local density approximation (LDA) FS. Further, while the measured areas of the different pockets, 0.15 holes ($T_c = 65$ K), 0.11 holes ($T_c = 45$ K), and 0.04 holes ($T_c = 0$ K)

are larger than the presumed doping levels, 0.11, 0.085, and <0.05, respectively, it is clear that the pocket size scales qualitatively with the doping level as predicted theoretically [6,10]. Interestingly, two fluid models of the pseudogap state do predict the observed discrepancy between the pocket size and carrier concentration or doping level [22]. The finding of a finite nodal FS rather than a "nodal" point at low T for the $T_c = 0$ K sample is at variance with recently reported findings under the same conditions [23]. The measured Fermi pockets are, however, in good agreement with those predicted by the YRZ ansatz. In Fig. 2(b) we show the spectral function calculated at E_F as a function of doping, where $A(\vec{k}, 0) = -(1/\pi)\,\mathrm{Im}G^{\mathrm{YRZ}}(\vec{k}, 0)$ and where $G^{\mathrm{YRZ}}(\vec{k}, 0)$ is Green's function taken from Ref. [6]. The experimental observations are remarkably well reproduced by this model with the doping level as the only adjustable parameter.

Turning to the question of whether the pocket areas are temperature dependent, we show in Fig. 3(a) the observed Fermi arc for the $T_c = 45$ K sample measured at three different temperatures: 60, 90, and 140 K, all in the normal state but well below T^*. The measured FS crossings in the figure are determined by the same method used in Figs. 1 and 2 rather than from the spectral weight at the Fermi level. In Fig. 3(b) we show the measured arc length as a function of temperature. It is clear that any change with temperature is minimal and certainly not consistent with an increase by more than a factor of 2 between the data taken at 140 and 60 K as would be expected by a T/T^* scaling of the arc length [21]. The discrepancy arises because previous experiments have not fully determined whether or not a band actually crosses the Fermi level.

The picture of the low energy excitations of the normal state emerging from the present study is of a nodal FS characterized by a Fermi "pocket" that, at temperatures above T_c, shows a minimal temperature dependence and an area proportional only to the doping level. We now turn our attention to the antinodal pseudogap itself.

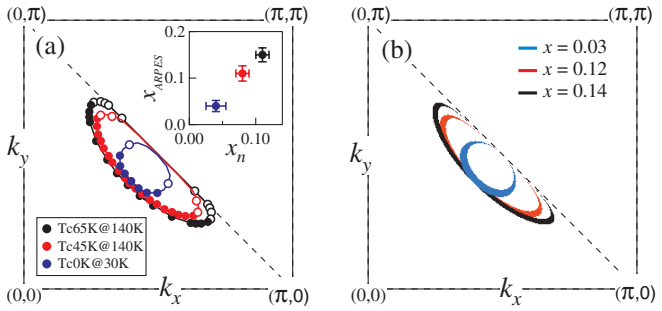

FIG. 2 (color online). (a) The pseudopockets determined for three different doping levels. The black data correspond to the $T_c = 65$ K sample, the blue data correspond to the $T_c = 45$ K sample, and the red data correspond to the nonsuperconducting $T_c = 0$ K sample. The area of the pockets x_{ARPES} scales with the nominal of doping level x_n, as shown in the inset. (b) The Fermi pockets derived from YRZ ansatz with different doping level.

Several theories of the pseudogap phase propose the formation of preformed singlet pairs above T_c in the antinodal region of the Brillouin zone [24]. The YRZ spin liquid based on the RVB picture is one such model as it recognizes the formation of resonating pairs of spin singlets along the copper-oxygen bonds of the square lattice as the lowest energy configuration. Figures 4(a)–4(d) show a series of spectral plots along the straight sector of the LDA FS in the antinodal region at a temperature of 140 K for the $T_c = 65$ K sample at the locations indicated in Fig. 4(e). Figure 4(f) shows intensity cuts through these plots along the horizontal lines indicated in Figs. 4(a)–4(d). It is evident that a symmetric gap exists at all points along this line. The particle-hole symmetry in binding energy observed here is in marked contrast to the particle-hole symmetry breaking predicted in the presence of density wave order and is a necessary condition for the formation of Cooper pairs. Thus the present observations add support to the hypothesis that the normal state is characterized by pair states forming along the copper-oxygen bonds and is consistent with earlier studies.

The combination of Figs. 2 and 4 points to a more complete picture of the low energy excitations in the normal state of the underdoped cuprates. For $T_c < T < T^*$, a Fermi pocket exists in the nodal region with an area proportional to the doping level. One does not need to invoke discontinuous Fermi arcs to describe the FS of underdoped Bi2212, and Luttinger's sum rule, properly understood, is seen to still approximately stand. However, as is evident in the inset of Fig. 2(a), the area of the hole pockets would appear to be larger than assumed doping level at the higher doping levels. This may reflect the presence of electron pockets at the higher doping level or it may reflect the presence of a bilayer splitting, even though the latter is not observed in the present study. We note that the splitting will be smaller in the underdoped region and in the nodal region. Although not verified in the present study, one

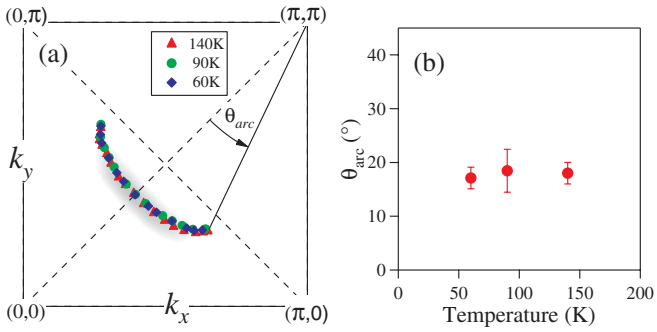

FIG. 3 (color online). (a) The Fermi surface crossings determined for the $T_c = 45$ K sample at three different temperatures. The triangles indicate measurements at a sample temperature of 140 K, the circles measurements at 90 K, and the diamonds measurements at 60 K. (b) The measured arc lengths in (a) plotted as a function of temperature. We note that rather than cycling the temperatures on the same sample, the data in (a) are measured on different samples cut from the same crystal.

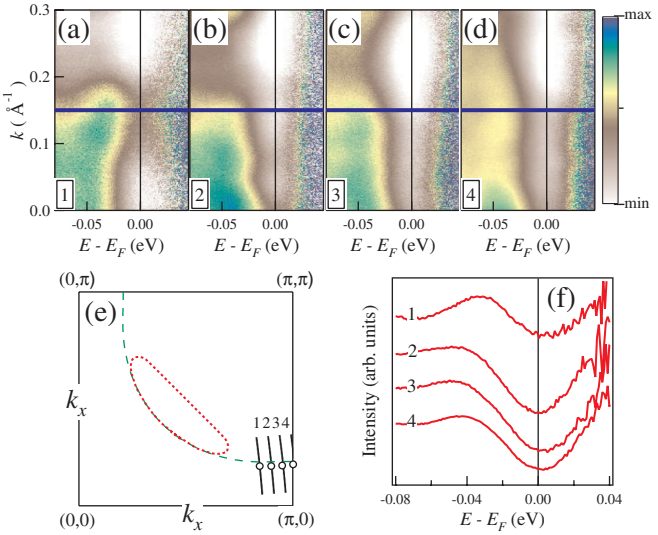

FIG. 4 (color online). (a)–(d) Spectra intensity measured at four points in the antinodal region as indicated in the schematic (e). The measurements are made with the sample in the normal state at a temperature of 140 K. (f) Intensity cuts through the spectral intensity maps of (a)–(d) as indicated by the lines in (a)–(d). They are also indicated by the open circles in (e).

assumes that, at some critical doping level greater than optimal, the reconstructed FS switches to the full Fermi surface as predicted in calculations [6,10]. The full FS ought to also be visible for $T > T^*$, as has been observed recently in ARPES measurements [25]. In the underdoped regime, as one moves away from the pockets, two further distinct regions exist as manifested in the spectral intensity. The region in the immediate vicinity of the end of the pockets is characterized by a gap that is asymmetric with respect to the chemical potential. This gap again reflects the underlying spin correlation in the system. In the antinodal region, the gap becomes symmetric with respect to the chemical potential and is therefore indicative of incoherent preformed pairs of electrons in singlet states. This picture of the FS appears to be entirely consistent with the momentum dependence of the gap function found in SISTS studies of the same material [26].

In conclusion, the photoemission measurements presented here show that the FS of the underdoped Bi2212 cuprate superconductors is defined not by disconnected arcs, but instead by fully closed hole pockets. The size and shape of these pockets are well reproduced within phenomenological models of the pseudogap state, such as the YRZ spin liquid, and are consistent with the doping in a Mott insulator. These results show the cuprates evolve with doping from an antiferromagnetic insulator into a pseudogap state characterized by a heavily renormalized band structure and strong pairing correlations reflecting the underlying structure of the lattice. These are the essential characteristics of the underdoped cuprates, the unraveling of which is prerequisite to understanding the ultimate emergence of superconductivity below T_c.

The authors would like to thank Seamus Davis, Mike Norman, Maurice Rice, John Tranquada, Alexei Tsvelik, Subir Sachdev, Tonica Valla, and Ali Yazdani for useful discussions. The work at Brookhaven is supported in part by the U.S. DOE under Contract No. DE-AC02-98CH10886 and in part by the Center for Emergent Superconductivity (CES), an Energy Frontier Research Center funded by the U.S. DOE, Office of Basic Energy Sciences. The work at Argonne is partially supported by the U.S. DOE under Contract No. DE-AC02-06CH11357 and partially by the same CES. T. E. Kidd acknowledges support from the Iowa Office of Energy Independence Grant No. 09-IPF-11.

[1] T. Timusk and B. Statt, Rep. Prog. Phys. **62**, 61 (1999).
[2] M. R. Norman *et al.*, Nature (London) **392**, 157 (1998).
[3] A. V. Chubukov and D. K. Morr, Phys. Rep. **288**, 355 (1997).
[4] S. Chakravarty, C. Nayak, and S. Tewari, Phys. Rev. B **68**, 100504 (2003).
[5] X. G. Wen and P. A. Lee, Phys. Rev. Lett. **80**, 2193 (1998).
[6] K. Y. Yang, T. M. Rice, and F. C. Zhang, Phys. Rev. B **73**, 174501 (2006).
[7] Y. Qi and S. Sachdev, Phys. Rev. B **81**, 115129 (2010).
[8] P. W. Anderson, Science **235**, 1196 (1987).
[9] K. Y. Yang *et al.*, Europhys. Lett. **86**, 37 002 (2009).
[10] J. P. F. LeBlanc, J. P. Carbotte, and E. J. Nicol, Phys. Rev. B **81**, 064504 (2010).
[11] A. J. H. Borne, J. P. Carbotte, and E. J. Nicol, Phys. Rev. B **82**, 024521 (2010).
[12] J. P. F. LeBlanc and J. P. Carbotte, arXiv:1006.5034.
[13] R. M. Konik, T. M. Rice, and A. M. Tsvelik, Phys. Rev. Lett. **96**, 086407 (2006).
[14] H.-B. Yang *et al.*, Nature (London) **456**, 77 (2008).
[15] J. Meng *et al.*, Nature (London) **462**, 335 (2009).
[16] N. Doiron-Leyraud *et al.*, Nature (London) **447**, 565 (2007).
[17] J. D. Rameau, H.-B. Yang, and P. D. Johnson, J. Electron Spectrosc. Relat. Phenom. **181**, 35 (2010).
[18] See Supplemental Material at http://link.aps.org/supplemental/10.1103/PhysRevLett.107.047003 for details of Fermi normalization and determination of FS crossing point.
[19] M. Granath and B. M. Andersen, Phys. Rev. B **81**, 024501 (2010).
[20] Y. Kohsaka *et al.*, Nature (London) **454**, 1072 (2008).
[21] A. Kanigel *et al.*, Nature Phys. **2**, 447 (2006).
[22] S. Chakraborty and P. Phillips, Phys. Rev. B **80**, 132505 (2009).
[23] U. Chatterjee *et al.*, Nature Phys. **6**, 99 (2009).
[24] V. J. Emery and S. A. Kivelson, Nature (London) **374**, 434 (1995).
[25] M. Hashimoto *et al.*, Nature Phys. **6**, 414 (2010).
[26] A. Pushp *et al.*, Science **324**, 1689 (2009).